JACS
JOURNAL OF THE AMERICAN CHEMICAL SOCIETY
pubs.acs.org/JACS

Article

Construction of Heteroleptic Copper Complexes in Perylene Diimide-Based COFs for Heterogeneous Metallaphotoredox Catalysis

Xia Wu, Jun Guo, Meng-Ying Sun, Tao Du, Debo Hao, Dongyi Liu, Deyang Wang, Songwei Wen, Jun Yin, Dan Li, and Jian He*

Cite This: https://doi.org/10.1021/jacs.5c17585

Read Online

ACCESS | Metrics & More | Article Recommendations | Supporting Information

ABSTRACT: Despite recent advances in developing diimine-containing copper photocatalysts for organic synthesis, further exploration of heteroleptic phenanthroline-ligated copper complexes remains challenging due to rapid ligand exchange in homogeneous solutions. Herein, we employ a framework-based heterogenization strategy to successfully synthesize such previously inaccessible copper complexes through postsynthetic modification. By integrating photoactive perylene diimide units into a one-dimensional covalent organic framework, the visible-light-driven oxo-azidation of styrenes can be accomplished with substantially reduced copper loadings in metallaphotoredox catalysis. Notably, our newly developed heterogeneous photocatalytic platform demonstrates that the reactive copper species facilitates the ketone formation step in the oxo-azidation without dissociation of one of the phenanthroline ligands. These findings highlight the potential of well-defined framework materials to address fundamental challenges in the synthesis of transition-metal complexes and enable detailed mechanistic studies that complement traditional homogeneous catalysis.

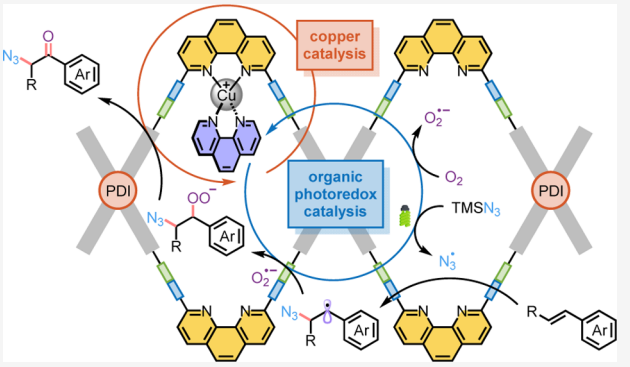

INTRODUCTION

In recent years, the development of efficient transition-metal catalysts utilizing the synergistic and confinement effects provided by framework-based supports has emerged as a promising approach to advancing synthetic methodologies.[1−8] Beyond enhancing catalyst stability and recyclability, the heterogenization of transition-metal species within crystalline porous frameworks alters their photophysical properties[9] and offers unique binding modes[10−12] that are difficult to achieve in homogeneous solutions. The generation of novel transition-metal complexes embedded in framework matrices, combined with their highly tunable coordination environments,[13−17] opens new opportunities for establishing more effective catalytic platforms and delving deeper insights into reaction mechanisms. Given the importance of sustainability and practicality in catalysis, as well as the challenges associated with improving the reactivity of first-row transition metals in conventional homogeneous systems,[18−20] developing robust heterogeneous catalysts[21−25] based on earth-abundant elements for organic synthesis[26,27] is highly desirable.

Owing to their exceptional single-electron transfer (SET) reactivity, copper-based catalysts have found extensive applications in radical-mediated processes under both thermal and photochemical conditions.[28−32] For instance, the pioneering work by Sauvage and co-workers on a homoleptic $[Cu(dap)_2]^+$ complex (where dap is 2,9-di(4-anisyl)-1,10-phenanthroline)[33] has enabled a diverse range of atom transfer radical addition (ATRA) reactions over the past decade,[34−38] with significant contributions from the Reiser group.[39−42] Introducing aryl substituents to the phenanthroline (phen) ligand in the Sauvage catalyst enhances photoactivity and stability through increased steric hindrance and $\pi-\pi$ stacking interactions (Scheme 1a).[43,44] However, it remains important to explore alternative phen-ligated copper complexes to further improve catalyst turnover numbers (TONs). We postulated that selective removal of the substituents from one of the two phen-based ligands could reduce steric congestion around the copper center, thereby improving substrate accessibility during redox processes while preserving weak $\pi-\pi$ stacking interactions (Scheme 1b). Such targeted ligand modification might produce more reactive copper species for photocatalytic reactions. Because 2,9-disubstituted and simple phen ligands have similar binding

Received: October 7, 2025
Revised: January 7, 2026
Accepted: January 12, 2026
Published: January 23, 2026

Scheme 1. Design of Stable Heteroleptic Phen-Ligated Copper Complexes for Heterogeneous Photocatalysis

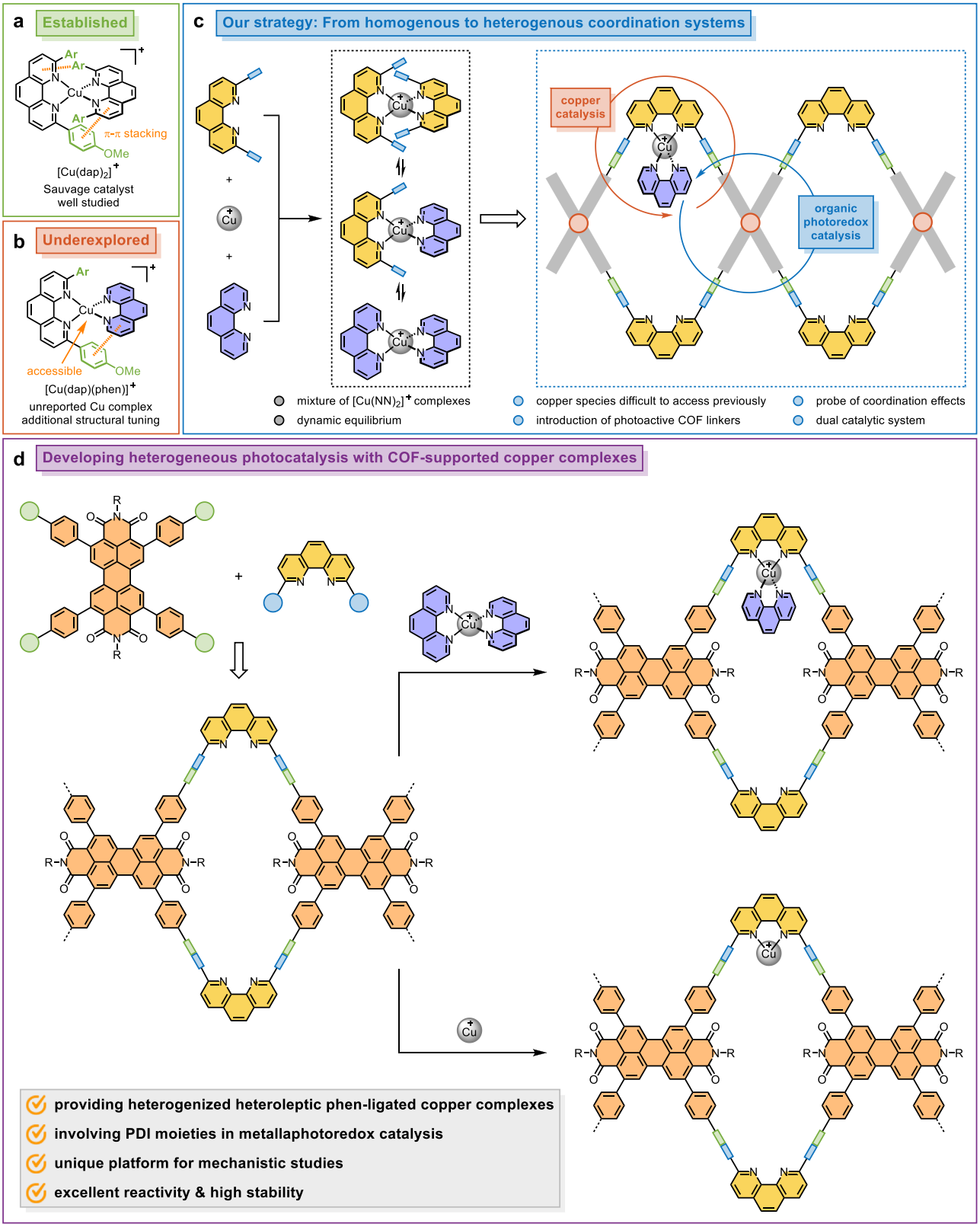

affinities, adding them to a homogeneous solution of cationic copper(I) consistently yields a mixture of homoleptic and heteroleptic phen-ligated complexes.[45] Given the rapid ligand exchange, the equilibria rarely favor copper species coordinated with two different phen-based ligands (Scheme 1c).

In order to suppress the formation of homoleptic phen-ligated copper(I) complexes via bimolecular pathways, we employ a strategy that incorporates 2,9-disubstituted phen moieties into a covalent organic framework (COF) solid support.[46−50] In this system, where copper active centers are effectively isolated, the

https://doi.org/10.1021/jacs.5c17585
J. Am. Chem. Soc. XXXX, XXX, XXX−XXX

Scheme 2. Schematic Representation of Catalyst Synthesis

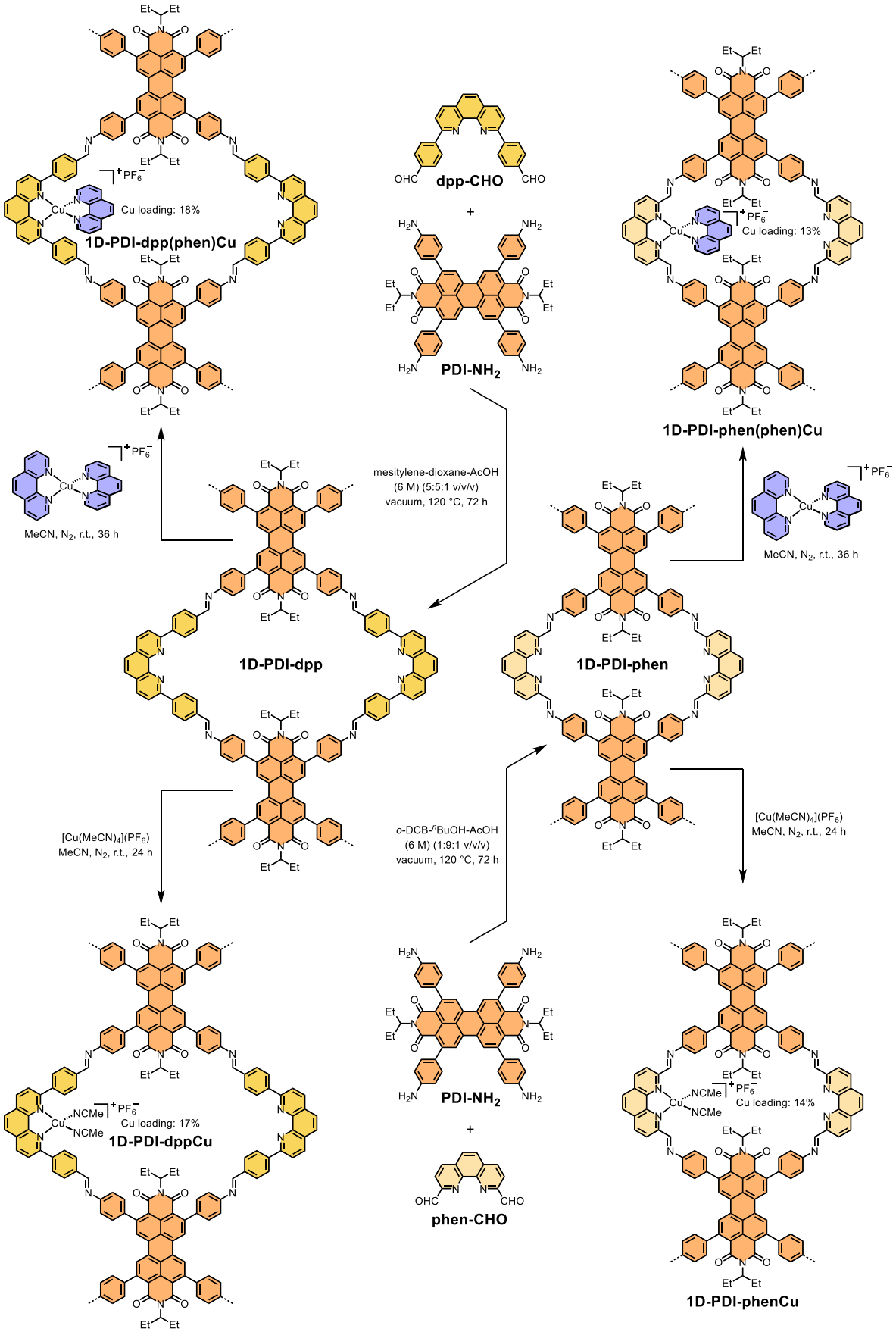

https://doi.org/10.1021/jacs.5c17585
J. Am. Chem. Soc. XXXX, XXX, XXX−XXX

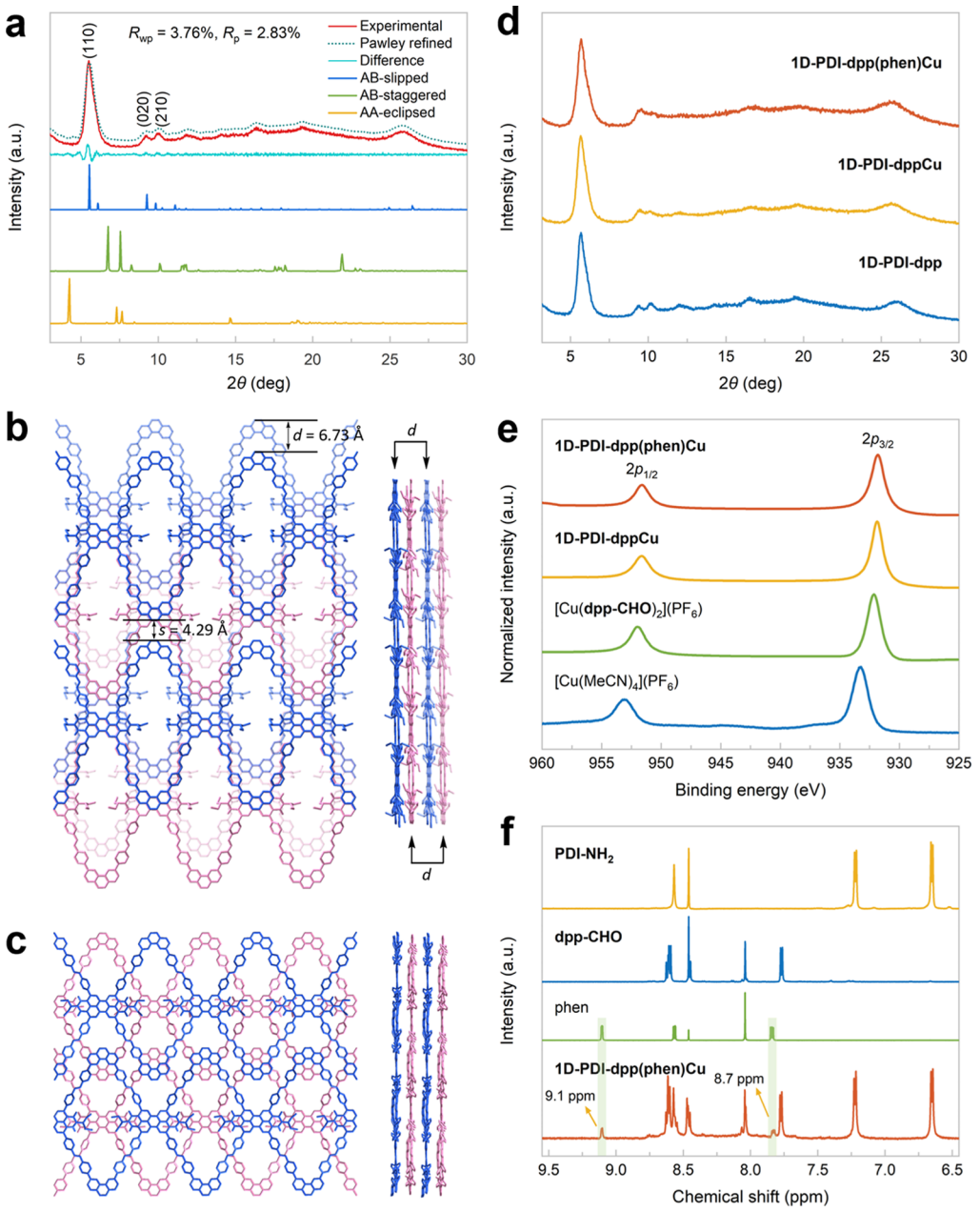

Figure 1. (a) PXRD patterns and refined modeling profiles of **1D-PDI−dpp**. (b) Simulated framework structure of the AB-slipped stacking mode viewed from the extended plane and along the 1D chain direction. (c) Simulated framework structure of the AB-staggered stacking mode. (d) Comparing PXRD patterns before and after postsynthetic metalation. (e) Cu2*p* XPS spectra showing the +1 oxidation state of the Cu centers in **1D-PDI−dpp(phen)Cu** and **1D-PDI−dppCu**. (f) NMR analysis of the digested sample of **1D-PDI−dpp(phen)Cu**.

dissociation of either a monophen-ligated copper(I) cation or a phen ligand from the immobilized heteroleptic complex is thermodynamically disfavored. Furthermore, restricted mass transfer within the COF pores helps stabilize the targeted complex by facilitating recombination after dissociation. As a result, the heterogeneous coordination environment effectively prevents the generation of the homoleptic $[Cu(phen)_2]^+$ complex, addressing an unresolved challenge present in comparable homogeneous systems. Due to the heterogenization of the phen-based ligand, a monophen-ligated copper complex can also form exclusively on the functional framework, which provides a well-defined platform to study ligand coordination effects in catalysis. Beyond accommodating phen moieties, crystalline COF materials can be tailored through presynthetic modification strategies to promote electron transfer under light irradiation.[51] By judiciously selecting the photoactive organic linkers, it is possible to design heterogeneous dual catalytic systems that merge copper catalysis with organic photoredox catalysis (Scheme 1c).

In this article, we present the synthesis of one-dimensional (1D) perylene diimide (PDI)-based COFs functionalized with phen moieties. Postsynthetic metalation with $[Cu(phen)_2]^+$ and cationic copper(I) yields COF-supported heteroleptic phen-ligated and monophen-ligated complexes, respectively (Scheme 1d). The integration of photoactive PDI units within the porous framework enables efficient generation of azide radicals upon photoexcitation,[52] thereby facilitating the oxo-azidation of styrenes using trimethylsilyl azide ($TMSN_3$) and O_2. Mecha-

https://doi.org/10.1021/jacs.5c17585
J. Am. Chem. Soc. XXXX, XXX, XXX−XXX

nistic studies provide new insights indicating that the heteroleptic phen-ligated copper complex, rather than the monophen-ligated counterpart, is the primary reactive species responsible for promoting ketone formation in the photocatalytic reaction. Through rational COF structure design, the heterogeneous copper catalyst outperforms its homogeneous analogues and can be recycled multiple times with minimal reactivity loss.

RESULTS AND DISCUSSION

Given the superior photoredox activity of PDI over pyrene units in nucleophile activation for ATRA,[52−55] we incorporated four aniline connecting moieties into the PDI core to create a tetra-amino-substituted organic linker (**PDI−NH$_2$**).[56] Drawing inspiration from the design of the Sauvage complex, we introduced two formyl groups in place of methoxy groups on the phen-based ligand to construct imine-linked COFs. Accordingly, we synthesized both 2,9-di(4-formylphenyl)-1,10-phenanthroline (**dpp−CHO**) and its phenyl-free analogue (**phen−CHO**), which were then employed to prepare the target PDI-based 1D framework materials (**1D-PDI−dpp** and **1D-PDI−phen**, respectively) under solvothermal conditions using different solvent combinations (Scheme 2). To ensure the formation of heteroleptic phen-ligated copper(I) complexes on the COF supports, we performed postsynthetic metalation by adding an acetonitrile solution of [Cu(phen)$_2$](PF$_6$) at room temperature. During immobilization on **1D-PDI−dpp** and **1D-PDI−phen**, one phen ligand dissociated from the copper center, resulting in heterogeneous heteroleptic copper photocatalysts (i.e., **1D-PDI−dpp(phen)Cu** and **1D-PDI−phen(phen)Cu**). Similarly, the corresponding catalysts containing monophen-ligated copper species, namely **1D-PDI−dppCu** and **1D-PDI−phenCu**, were prepared by treating the COF supports with [Cu(MeCN)$_4$](PF$_6$). Due to its smaller pore size, the copper loadings in **1D-PDI−phen** were lower than those in **1D-PDI−dpp**. Moreover, the incorporation of the relatively bulky heteroleptic phen-ligated copper complex in **1D-PDI−phen** reduced its crystallinity, which could potentially lead to metal leaching during catalysis (Figure S1). Similarly, replacing [Cu(phen)$_2$](PF$_6$) with more sterically hindered [Cu(dmp)$_2$](PF$_6$) (where dmp is 2,9-dimethyl-1,10-phenanthroline) resulted in dramatic decrease in metalation efficiency (Table S1). Therefore, we primarily focused on **1D-PDI−dpp(phen)Cu** for detailed characterization and photocatalytic investigations.

In addition to employing FT-IR and solid-state ^{13}C NMR to analyze the chemical composition of **1D-PDI−dpp** (Figures S2 and S3), we examined its crystallinity using powder X-ray diffraction (PXRD) techniques (Figure 1a). The PXRD patterns displayed a prominent peak at 5.51°, along with two relatively weak peaks around 10°, corresponding to the (110), (020), and (210) reflection planes in a distinctive AB-slipped stacking mode. The Pawley-refined PXRD profiles showed excellent agreement with the experimental data, providing R_{wp} and R_p values of 3.76% and 2.83%, respectively. Similar to other stacking modes, the extended planes formed by the 1D chains adopt a parallel arrangement. However, to achieve overlap between the nearest planes (highlighted in blue or pink) following a perpendicular shift, a slip operation, vertical to the chain with a displacement (d) of 6.73 Å, is necessary (Figure 1b). The closest chains on two neighboring planes are offset by half a repeating unit along the 1D chain direction, same as those simulated in the COF structure of the AB-staggered stacking mode (Figure 1c). Notably, both the AB-staggered and AA-eclipsed modes show alternating adjacent chains within the same plane (Figures 1c and S4), giving small interstitial pores that are inconsistent with the PXRD results. In contrast, the simulated structure with the AB-slipped stacking features chains arranged in parallel, with an interchain separation (s) of 4.29 Å, which corresponds to the value of d minus the distance between two parallel C−C bonds in a benzene ring (Figure 1b). This dramatic change in chain assembly within the extended plane is most likely driven by the strong $\pi-\pi$ stacking interactions between the PDI core and the phen moieties from the upper and lower COF layers (Figure S5). Unlike 1D COFs built from pyrene-based organic linkers,[57−59] the PDI units in **1D-PDI−dpp** experience greater dipole repulsion from the diimide motifs and steric hindrance from the *N*-alkyl substituents,[60] both of which disfavor the AA-eclipsed stacking mode (Figure S4). While both the AB-slipped and AB-staggered stacking modes alleviate these repulsive interactions, the additional stabilization from the $\pi-\pi$ stacking results in **1D-PDI−dpp** adopting a triclinic rather than an orthorhombic crystal system (Figure S5a and Table S2).

Scanning electron microscopy analysis showed that the morphology of **1D-PDI−dpp** remained intact after postsynthetic metalation with [Cu(phen)$_2$](PF$_6$) or [Cu(MeCN)$_4$](PF$_6$) (Figures S6−S8). The crystallinity was also preserved, as indicated by the PXRD patterns (Figure 1d). Furthermore, energy-dispersive X-ray spectroscopy mapping revealed a homogeneous distribution of the elements C, N, O, and Cu throughout the framework, which confirmed the consistent composition of both **1D-PDI−dpp(phen)Cu** and **1D-PDI−phen(phen)Cu** (Figures S11 and S12). The Cu2$p_{1/2}$ and Cu2$p_{3/2}$ peaks observed in the X-ray photoelectron spectroscopy (XPS) spectra of the COF-supported photocatalysts can be attributed to copper(I) species (Figure 1e). The shifts toward lower binding energies are due to the coordination of phenanthroline ligands to the copper center.[9] It is noteworthy that XPS analysis revealed mixed-valence states of copper in [Cu(**dpp−CHO**)(MeCN)$_2$](PF$_6$) (Figure S13), confirming that the COF support effectively prevents the oxidation of monophen-ligated copper(I) species in air (Figure 1e). The digestion of **1D-PDI−dpp(phen)Cu** with trifluoroacetic acid, followed by the addition of sodium cyanide, produced characteristic peaks of free phen as well as signals from the organic linkers (Figure 1f). The integration of the phen ligand closely correlated with the copper content in the COF-supported catalyst, suggesting the successful formation of the targeted heteroleptic phen-ligated copper complex within the framework pores (Figure S16 and Table S3).

To efficiently produce α-azido ketones, an important class of versatile synthetic intermediates,[61] via heterogeneous photocatalysis, we employed **1D-PDI−dpp(phen)Cu** as the catalyst to explore the oxo-azidation of simple styrene with TMSN$_3$ in air under light irradiation (Table S4).[40] Following a systematic evaluation of light wavelengths and solvents, we established that a robust photocatalytic system could deliver 2-azido-1-phenylethanone (**1**) in 78% yield using just 0.1 mol % of **1D-PDI−dpp(phen)Cu** and green LED lamps as the light source (Table 1, entry 1). Control experiments demonstrated that the oxo-azidation reaction did not proceed in the absence of catalyst, light, or air (Table S4, entries 2−5). Moreover, no styrene was consumed under the irradiation conditions without **1D-PDI−dpp(phen)Cu**, indicating that benzaldehyde side product was generated photocatalytically. Notably, when the phen ligand was removed from the immobilized copper active center, the yield of

https://doi.org/10.1021/jacs.5c17585
J. Am. Chem. Soc. XXXX, XXX, XXX−XXX

Table 1. Effect of Different Copper Photocatalytic Systems on the Oxo-Azidation of Styrene[a]

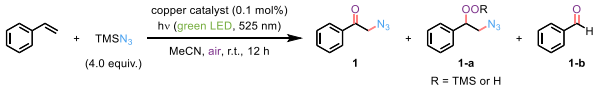

entry	catalyst	yield of **1** (%)	yield of **1-a** (%)	yield of **1-b** (%)	conversion of styrene (%)
1	**1D-PDI−dpp(phen)Cu**	78	<5	21	>95
2	**1D-PDI−dppCu**	32	31	9	81
3[b]	**1D-PDI−dpp**	20	40	17	95
4[b,c]	**1D-PDI−dpp**	23	36	19	>95
5[b]	**PDI−NH$_2$**	<5	<5	<5	5
6[b]	**dpp−CHO**	<5	<5	<5	10
7	**1D-PDI−phen(phen)Cu**	34	7	8	50
8	**1D-PDI−phenCu**	21	11	<5	39
9	**1D-Py−dpp(phen)Cu**	17	27	8	64
10	**1D-Py−dppCu**	8	13	7	30
11	**1D-Py−phen(phen)Cu**	12	22	8	52
12	**1D-Py−phenCu**	7	8	<5	26
13	[Cu(phen)$_2$](PF$_6$)	<5	6	<5	14
14	[Cu(**dpp−CHO**)$_2$](PF$_6$)	<5	10	<5	16
15	[Cu(**L**)$_2$](PF$_6$)	12	36	6	52
16	[Cu(phen)(xantphos)](PF$_6$)	<5	<5	<5	<5
17	[Cu(phen)(binap)](PF$_6$)	<5	15	<5	23
18	(binap)$_2$Cu$_2$I$_2$	6	13	<5	21

[a]Reaction conditions: styrene (0.10 mmol, 1.0 equiv), $TMSN_3$ (4.0 equiv), and copper catalyst (0.1 mol %) in acetonitrile (0.4 mL) under air atmosphere at room temperature with green-LED light irradiation (525 nm) for 12 h. Xantphos, (9,9-dimethyl-9*H*-xanthene-4,5-diyl) bis(diphenylphosphane); binap, 2,2′-bis-(diphenylphosphino)-1,1′-binaphthyl. Yield and conversion were determined by ^{1}H NMR of the crude reaction mixture using 1,1,2,2-tetrachloroethane as an internal standard. [b]The amount of the framework or organic linker used was the same as that in the case of **1D-PDI−dpp(phen)Cu**. [c]Reaction time was extended to 24 h.

product **1** decreased to 32%, while a comparable amount of peroxide **1-a** was obtained (Table 1, entry 2). In the meantime, the overall conversion of styrene declined to 81%. Using the parent framework support (i.e., **1D-PDI−dpp**) as the photocatalyst, despite achieving high substrate conversion, the desired product yield further dropped to 20% (Table 1, entry 3). Extending the reaction time did not promote the conversion of **1-a** to **1** (Table 1, entry 4), which demonstrates the crucial role of the copper active center in facilitating the oxo-azidation of styrene. The PDI or phen linker alone exhibited fairly low activity, underscoring the importance of framework construction in this photocatalytic system (Table 1, entries 5 and 6). It is worth noting that the employment of **1D-PDI−phen** as the solid support reduced both the product yield and overall conversion (Table 1, entries 7 and 8). Recycled **1D-PDI−phen(phen)Cu**, which showed diminished PXRD signals consistent with the trend observed in freshly prepared **1D-PDI−phen**-based catalysts via postsynthetic metalation (Figure S1), further decreased the yield of product **1** to 17% in the second run (Table S8 and Figure S34). This indicates that **1D-PDI−phen** is not a suitable matrix for hosting heteroleptic phen-ligated copper complexes in photocatalytic applications. Nevertheless, their performance remained superior to that of copper catalysts embedded in well-established pyrene-based COFs[62−64] (Table 1, entries 9−12), demonstrating the benefits of incorporating photoactive PDI units into catalyst design. Very importantly, across all four framework supports tested, the heteroleptic phen-ligated copper complexes consistently outperformed their monophen-ligated counterparts (Table 1, entries 1, 2, and 7−12). Regarding the survey of homogeneous copper photocatalysis, while conventional Sauvage-type catalysts showed low reactivity at a copper loading of 0.1 mol % (Table 1, entries 13 and 14), mixing the simple phen ligand with **dpp−CHO** in a 1:1 ratio in the presence of [Cu(MeCN)$_4$](PF$_6$) markedly increased the yields of compounds **1** and **1-a** (Table 1, entry 15). Such findings provide strong evidence that heteroleptic phen-ligated copper complexes can function as promising catalysts for photoinduced oxo-azidation reactions. In addition, phosphine-based monomeric and dimeric copper photocatalysts proved to be ineffective and were excluded from the heterogenization approach (Table 1, entries 16−18).[45,65,66]

With the optimized conditions established, we explored the scope of styrene substrates in the heterogeneous photocatalytic

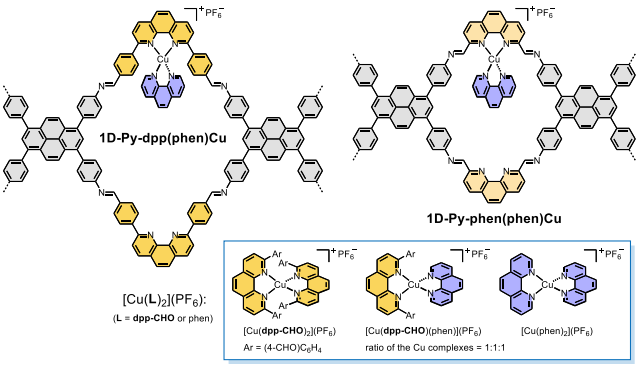

oxo-azidation (Table 2). Both electron-donating and electron-withdrawing functional groups at various positions on the aryl ring were well tolerated, furnishing α-azido ketones in synthetically useful yields (products **1**−**18**). The copper catalyst achieved a turnover number (TON) of up to 760, surpassing the performance of existing homogeneous and heterogeneous systems (Table S5). The high compatibility with nitrogen-containing functionalities and halogen atoms demonstrated the robustness of the current methodology for chemical synthesis (products **6** and **11**−**17**). In addition to achieving higher TONs compared to conventional copper catalysis (Table S6), the use of highly electron-rich 2-methoxy-4-vinylphenol, which was previously incompatible with the homogeneous catalytic system,[67] successfully yielded the α-azido ketone (**18**) with only 0.1 mol % of **1D-PDI−dpp(phen)Cu**. Furthermore, the substrate scope could be further expanded to include naphthalene and heterocycles such as pyridines, indoles, and thiophenes (products **19**−**22**). Notably, while allylbenzene and trisubstituted alkenes were not suitable for oxo-azidation, the use of β-methylstyrene, an internal alkene, afforded desired product **23** in 45% yield. The double bond functionalization process is also applicable to the alkenes derived from complex bioactive molecules (products **24** and **25**), including estrone and formononetin. Moreover, this heterogeneous photocatalysis can be employed in a variety of alkene difunctionalization reactions with low copper loadings (Figures S27−S31), underscoring its versatility and promising potential for practical applications in organic synthesis.

Compared to **1D-PDI−phen(phen)Cu**, which showed significantly reduced activity and lower signal intensity in PXRD measurements after the first catalytic run (Table S8 and

https://doi.org/10.1021/jacs.5c17585
J. Am. Chem. Soc. XXXX, XXX, XXX−XXX

Table 2. Substrate Scope of Heterogeneous Photocatalytic Oxo-Azidation[a]

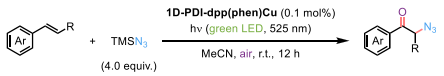

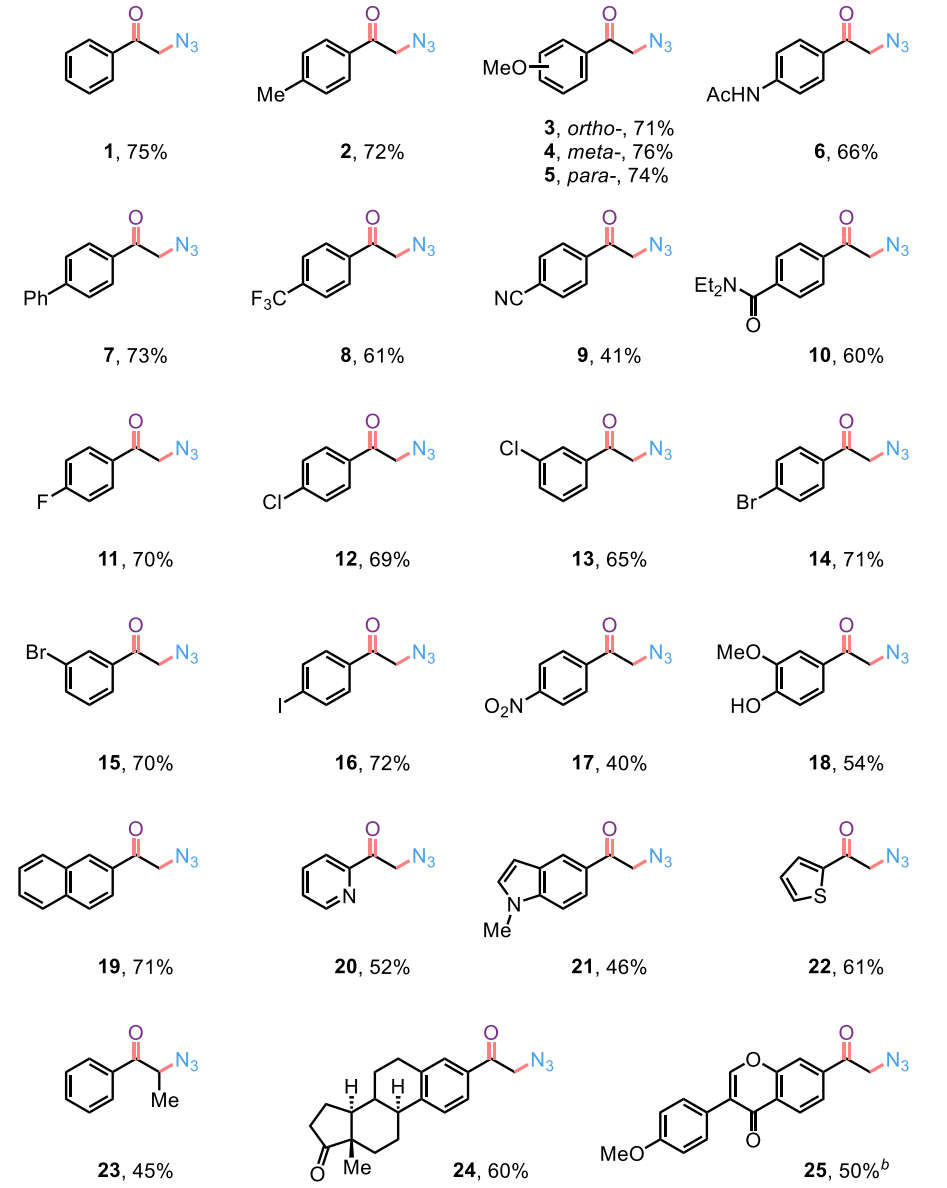

[a]Reaction conditions: styrene derivative (0.10 mmol, 1.0 equiv), $TMSN_3$ (4.0 equiv), and **1D-PDI−dpp(phen)Cu** (0.1 mol %) in acetonitrile (0.4 mL) under air atmosphere at room temperature with green-LED light irradiation (525 nm) for 12 h. Data are reported as isolated yields. [b]Dichloromethane was used as the solvent instead, due to the substrate's high solubility.

Figure S34),[68] the optimal catalyst assembled from **dpp−CHO** and **PDI−NH_2** demonstrated excellent recyclability (Figure 2a,b). The template oxo-azidation reaction delivered product **1** with a 70% isolated yield in the fourth run, alongside well-preserved PXRD patterns of the framework. XPS analysis revealed that the heterogenized heteroleptic phen-ligated copper complex was partially oxidized to copper(II)[69] during the photoredox catalysis in air (Figure 2c). Critically, ICP and NMR analyses of the digested samples evidenced no leaching of copper or the phen ligand, supporting the role of this heteroleptic complex as the actual catalytic species (Figure 2d and Table S3). To further elucidate the details of the heterogeneous photocatalytic process involving the photoactive framework support, we performed electron paramagnetic resonance (EPR) experiments using 5,5-dimethyl-1-pyrroline *N*-oxide (DMPO) as the radical trapping reagent (Figure 2e,f). Under a nitrogen atmosphere, green light irradiation triggered the formation of a DMPO−N_3 adduct,[70] demonstrating that photoexcited **1D-PDI−dpp** can effectively extract an electron from $TMSN_3$ to generate an azide radical. However, the expected photoluminescent quenching of **1D-PDI−dpp** in the presence of $TMSN_3$ was not observed (Figure S35), likely due to self-quenching effects within the COF layers. On the other hand, when the atmosphere was switched to air, the EPR signals clearly

https://doi.org/10.1021/jacs.5c17585
J. Am. Chem. Soc. XXXX, XXX, XXX−XXX

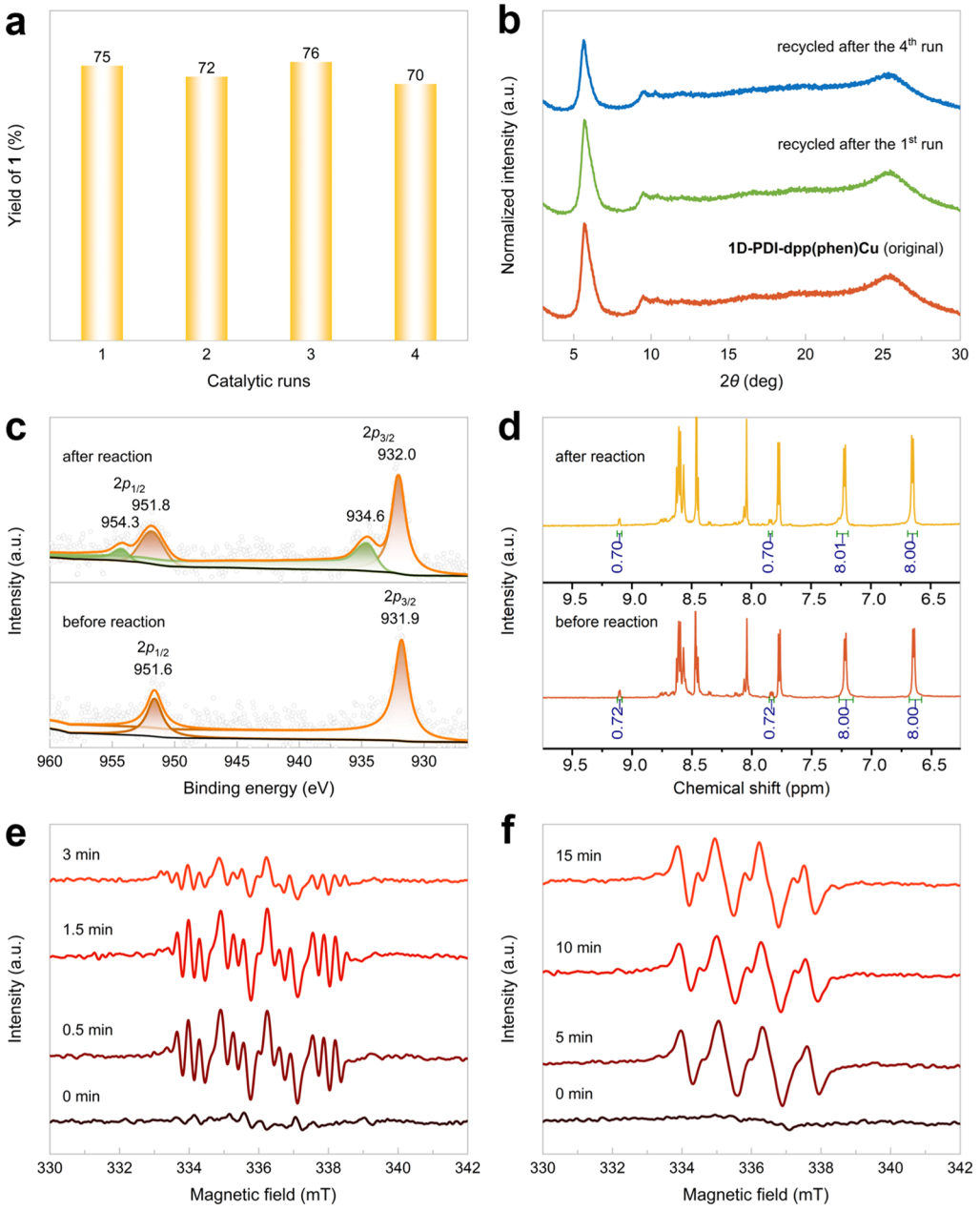

Figure 2. (a) Recycling experiments for photocatalytic oxo-azidation of styrene. (b) PXRD patterns of the original (orange line) and recycled **1D-PDI−dpp(phen)Cu** after one run (green line) and four runs (blue line). (c) Cu2*p* XPS spectra of **1D-PDI−dpp(phen)Cu** before and after oxo-azidation. (d) ^{1}H NMR spectra of digested **1D-PDI−dpp(phen)Cu** samples before and after oxo-azidation. (e) X-band EPR spectra (9.43 GHz, 298 K) of **1D-PDI−dpp**, DMPO, and $TMSN_3$ in acetonitrile under nitrogen atmosphere, recorded under irradiation (525 nm) for 0−3 min. (f) X-band EPR spectra (9.43 GHz, 298 K) of **1D-PDI−dpp**, DMPO, and $TMSN_3$ in acetonitrile under air atmosphere, recorded under irradiation (525 nm) for 0−15 min.

revealed distinct peaks corresponding to a DMPO−O_2^- adduct after 5 min of irradiation.[71] This suggests that the superoxide ion was most likely produced through electron transfer between reduced **1D-PDI−dpp** and O_2.

To clarify the role of the immobilized copper species in the oxo-azidation, we removed the framework catalyst and benzaldehyde (**1-b**) from the reaction mixture by simple filtration through a short pad of silica gel, followed by evacuation (Figure 3a). Subsequently, we mimicked the original photocatalytic conditions by reintroducing $TMSN_3$ and various types of COF-based catalysts into the mixture of compounds **1** and **1-a** in acetonitrile under air atmosphere. Control experiments were conducted in parallel without light exposure. Not surprisingly, the addition of **1D-PDI−dpp** did not lead to any further formation of product **1**. Peroxide **1-a** was not photochemically stable; it gradually decomposed and produced benzaldehyde upon light irradiation. These results demonstrate that the framework support itself is incapable of converting **1-a** to **1**. Using **1D-PDI−dppCu** as the catalyst slightly increased the yield of product **1**, from 20% to 25% in the absence of light and to 28% in its presence. The poor mass balance observed under green LED light again reflected the photochemical instability of peroxide **1-a**. Notably, the complete consumption of peroxide **1-a** was confirmed when **1D-PDI−dpp(phen)Cu** was employed. Substantial amounts of product **1** were obtained regardless of light irradiation, indicating that the heteroleptic phen-ligated

https://doi.org/10.1021/jacs.5c17585
J. Am. Chem. Soc. XXXX, XXX, XXX−XXX

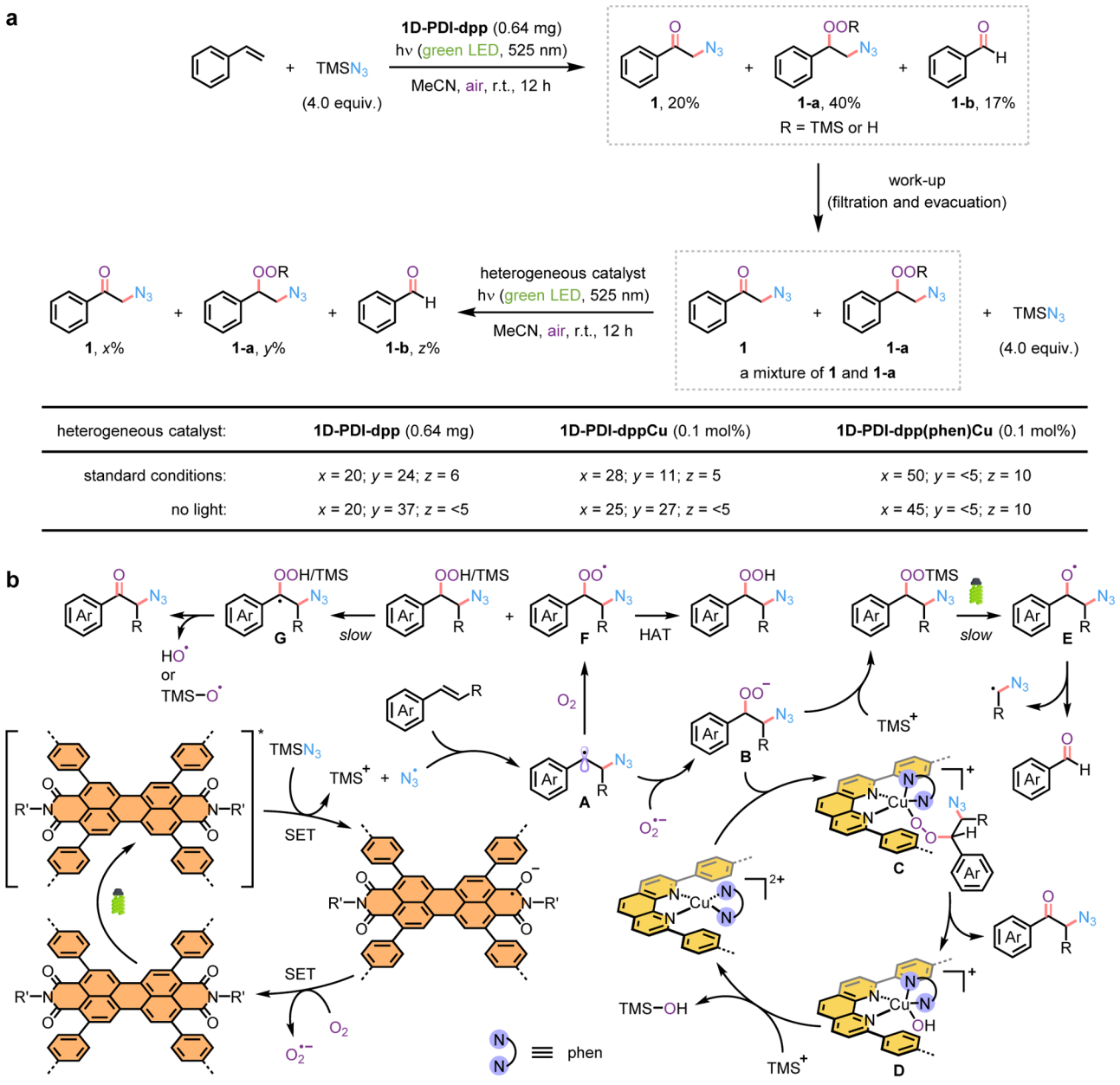

heterogeneous catalyst:	**1D-PDI-dpp** (0.64 mg)	**1D-PDI-dppCu** (0.1 mol%)	**1D-PDI-dpp(phen)Cu** (0.1 mol%)
standard conditions:	x = 20; y = 24; z = 6	x = 28; y = 11; z = 5	x = 50; y = <5; z = 10
no light:	x = 20; y = 37; z = <5	x = 25; y = 27; z = <5	x = 45; y = <5; z = 10

Figure 3. (a) Investigating the transformations of side-product **1-a** in the presence of different COF-based catalysts. Data are reported as crude ^{1}H NMR yields, calculated with styrene as the limiting reagent. (b) Plausible mechanism for oxo-azidation of styrene derivatives with **1D-PDI–dpp(phen)Cu**. HAT, hydrogen atom transfer.

copper complex on the framework support acts as the active site for the transformation of **1-a** into **1**. This nonphotoinduced process occurred rapidly enough to prevent the photochemical decomposition of peroxide **1-a**. Initial rate analysis revealed that the reaction follows first-order kinetics with respect to both **1-a** and **1D-PDI–dpp(phen)Cu** (Figures S36–S39). Furthermore, **1D-PDI–dppCu** was found to be considerably less effective (Figure S40), aligning with the observed trends in the studies of Cu^{2+} and phen ratios for the corresponding homogeneous catalytic system (Table S9).

A comprehensive mechanistic understanding, obtained through materials characterization, EPR spectroscopy, and well-designed control experiments, enabled us to propose the reaction pathways for the heterogeneous metallaphotoredox catalysis depicted in Figure 3b. When exposed to green LED light, the photoexcited PDI unit in **1D-PDI–dpp** undergoes SET with $TMSN_3$, generating a PDI radical anion, TMS^+, and an azide radical. The nitrogen-centered radical then reacts with styrene via radical addition, forming a more stable benzylic radical(**A**). The superoxide ion, provided by the single-electron reduction of O_2 by the PDI radical anion, couples with intermediate **A** through radical recombination to form a β-azido peroxide (**B**). The COF-supported, heteroleptic phen-ligated copper(II) complex utilizes its vacant coordination sites to capture intermediate **B**, yielding a five- or six-coordinate copper–alkylperoxo adduct (**C**), which rapidly affords the desired oxo-azidation product and hydroxide-ligated copper complex **D**. Subsequently, trapping with TMS^+ produces a strong Si–O bond and regenerates the cationic copper(II) catalyst, thereby closing the catalytic cycle.

In addition to the primary reaction pathway, parallel radical mechanisms operate. First, intermediate **B** can be trapped by

https://doi.org/10.1021/jacs.5c17585
J. Am. Chem. Soc. XXXX, XXX, XXX–XXX

TMS^+ to form a silyl-substituted peroxide. Upon light irradiation, this peroxide undergoes homolytic O−O bond cleavage to generate a benzyloxy radical (**E**), which then fragments via β-scission of its C−C bond to yield benzaldehyde. Simultaneously, intermediate **A** gradually reacts with O_2 to form a benzyl peroxide radical intermediate (**F**). This highly reactive species can abstract a hydrogen atom either from a solvent molecule to form a hydrogen peroxide derivative or from the benzylic position of peroxide side products at a slow rate, leading to an alkyl radical intermediate (**G**) adjacent to a peroxide group. A final homolytic cleavage of the O−O bond in intermediate **G** delivers the desired product via a noncopper-catalyzed pathway, along with an oxygen-centered radical. Obviously, in the absence of intermediate **F**, the peroxide side products cannot be converted to the desired oxo-azidation product without the assistance of the copper active center bearing two different phen-type ligands.

CONCLUSIONS

In the current study, we report the synthesis and characterization of a heteroleptic phen-ligated copper complex embedded within a stable PDI-based covalent organic framework featuring a unique AB-slipped stacking mode. Compared to the corresponding monophen-ligated copper complex and its pyrene-based 1D framework-supported counterparts, this recyclable heterogeneous copper photocatalyst exhibits superior activity in the oxo-azidation of styrenes with $TMSN_3$ under air atmosphere. Mechanistic investigations reveal that the ketone formation step in the three-component radical-mediated process is facilitated by the copper active center containing two phen ligands, rather than one —a critical insight unattainable in conventional homogeneous photocatalytic systems. Further applications in heterogeneous metallaphotoredox catalysis are currently underway in our laboratory.

ASSOCIATED CONTENT

Supporting Information

The Supporting Information is available free of charge at https://pubs.acs.org/doi/10.1021/jacs.5c17585.

The Supporting Information is available free of charge via the internet at. Experimental details for the preparation and characterization of COFs, catalysis, and additional data (PDF)

AUTHOR INFORMATION

Corresponding Author

Jian He − *Department of Chemistry, The University of Hong Kong, Hong Kong 999077, China; State Key Laboratory of Synthetic Chemistry and Shanghai-Hong Kong Joint Laboratory in Chemical Synthesis, The University of Hong Kong, Hong Kong 999077, China; Materials Innovation Institute for Life Sciences and Energy (MILES), HKU-SIRI, Shenzhen 518048, China;* orcid.org/0000-0002-3388-3239; Email: jianhe@hku.hk

Authors

Xia Wu − *Department of Chemistry, The University of Hong Kong, Hong Kong 999077, China*

Jun Guo − *Department of Chemistry, The University of Hong Kong, Hong Kong 999077, China; State Key Laboratory of Synthetic Chemistry and Shanghai-Hong Kong Joint Laboratory in Chemical Synthesis, The University of Hong Kong, Hong Kong 999077, China;* orcid.org/0000-0003-4170-2853

Meng-Ying Sun − *Department of Chemistry, The University of Hong Kong, Hong Kong 999077, China; Materials Innovation Institute for Life Sciences and Energy (MILES), HKU-SIRI, Shenzhen 518048, China*

Tao Du − *Department of Applied Physics, The Hong Kong Polytechnic University, Kowloon 999077, China;* orcid.org/0000-0003-2402-6320

Debo Hao − *Guangdong Provincial Key Laboratory of Supramolecular Coordination Chemistry, Jinan University, Guangzhou 510632, China*

Dongyi Liu − *Department of Chemistry, The University of Hong Kong, Hong Kong 999077, China*

Deyang Wang − *Department of Chemistry, The University of Hong Kong, Hong Kong 999077, China; State Key Laboratory of Synthetic Chemistry and Shanghai-Hong Kong Joint Laboratory in Chemical Synthesis, The University of Hong Kong, Hong Kong 999077, China*

Songwei Wen − *Department of Chemistry, The University of Hong Kong, Hong Kong 999077, China*

Jun Yin − *Department of Applied Physics, The Hong Kong Polytechnic University, Kowloon 999077, China;* orcid.org/0000-0002-1749-1120

Dan Li − *Guangdong Provincial Key Laboratory of Supramolecular Coordination Chemistry, Jinan University, Guangzhou 510632, China;* orcid.org/0000-0002-4936-4599

Complete contact information is available at: https://pubs.acs.org/10.1021/jacs.5c17585

Notes

The authors declare no competing financial interest.

ACKNOWLEDGMENTS

The authors gratefully acknowledge the National Natural Science Foundation of China (grant nos. 22422109 and 22201236 to J.H.), the Research Grants Council of the Hong Kong Special Administrative Region, People's Republic of China (grant nos. 17310925 to J.H.; 25300823 and 15300724 to J.Y.), the Croucher Foundation, the Innovation and Technology Commission (HKSAR, China), Materials Innovation Institute for Life Science and Energy (MILES), The University of Hong Kong, and the Guangdong Major Project of Basic and Applied Research (2019B030302009) for their financial support.

REFERENCES

(1) Yang, Q.; Xu, Q.; Jiang, H.-L. Metal−Organic Frameworks Meet Metal Nanoparticles: Synergistic Effect for Enhanced Catalysis. *Chem. Soc. Rev.* **2017**, *46*, 4774−4808.

(2) Huang, Y.-B.; Liang, J.; Wang, X.-S.; Cao, R. Multifunctional Metal−Organic Framework Catalysts: Synergistic Catalysis and Tandem Reactions. *Chem. Soc. Rev.* **2017**, *46*, 126−157.

(3) Drake, T.; Ji, P.; Lin, W. Site Isolation in Metal−Organic Frameworks Enables Novel Transition Metal Catalysis. *Acc. Chem. Res.* **2018**, *51*, 2129−2138.

(4) Lee, J.-S. M.; Cooper, A. I. Advances in Conjugated Microporous Polymers. *Chem. Rev.* **2020**, *120*, 2171−2214.

(5) Liu, J.; Goetjen, T. A.; Wang, Q.; Knapp, J. G.; Wasson, M. C.; Yang, Y.; Syed, Z. H.; Delferro, M.; Notestein, J. M.; Farha, O. K.; Hupp, J. T. MOF-Enabled Confinement and Related Effects for

https://doi.org/10.1021/jacs.5c17585
J. Am. Chem. Soc. XXXX, XXX, XXX−XXX

Chemical Catalyst Presentation and Utilization. *Chem. Soc. Rev.* **2022**, *51*, 1045−1097.
(6) Chen, W.; Cai, P.; Zhou, H.-C.; Madrahimov, S. T. Bridging Homogeneous and Heterogeneous Catalysis: Phosphine-Functionalized Metal-Organic Frameworks. *Angew. Chem., Int. Ed.* **2024**, *63*, No. e202315075.
(7) Jin, H.-G.; Zhao, P.-C.; Qian, Y.; Xiao, J.-D.; Chao, Z.-S.; Jiang, H.-L. Metal−Organic Frameworks for Organic Transformations by Photocatalysis and Photothermal Catalysis. *Chem. Soc. Rev.* **2024**, *53*, 9378−9418.
(8) Song, Y.; Ma, S. Pore Engineering in Metal−Organic Frameworks and Covalent Organic Frameworks: Strategies and Applications. *Chem. Sci.* **2025**, *16*, 11740−11767.
(9) Guo, J.; Xia, Q.; Tang, W. Y.; Li, Z.; Wu, X.; Liu, L.-J.; To, W.-P.; Shu, H.-X.; Low, K.-H.; Chow, P. C. Y.; Lo, T. W. B.; He, J. Visible Light-Mediated Intermolecular Crossed [2 + 2] Cycloadditions Using a MOF-Supported Copper Triplet Photosensitizer. *Nat. Catal.* **2024**, *7*, 307−320.
(10) Sawano, T.; Thacker, N. C.; Lin, Z.; McIsaac, A. R.; Lin, W. Robust, Chiral, and Porous BINAP-Based Metal−Organic Frameworks for Highly Enantioselective Cyclization Reactions. *J. Am. Chem. Soc.* **2015**, *137*, 12241−12248.
(11) Ma, B.; Xia, Q.; Wang, D.; Jin, J.-K.; Li, Z.; Liang, Q.-J.; Sun, M.-Y.; Liu, D.; Liu, L.-J.; Shu, H.-X.; Yang, J.; Li, D.; He, J. Metal-Organic Framework Supported Copper Photoredox Catalysts for Iminyl Radical-Mediated Reactions. *Angew. Chem., Int. Ed.* **2023**, *62*, No. e202300233.
(12) Chen, J.-R.; Zhou, D.; Liu, Y.; Li, M.; Xiao, Y.; Huang, X.-C.; Che, C.-M. Luminescent Cyclometalated Gold(III) Complexes Covalently Linked to Metal−Organic Frameworks for Heterogeneous Photocatalysis. *Chem. Sci.* **2025**, *16*, 2202−2214.
(13) Wu, C.-D.; Zhao, M. Incorporation of Molecular Catalysts in Metal−Organic Frameworks for Highly Efficient Heterogeneous Catalysis. *Adv. Mater.* **2017**, *29*, 1605446.
(14) Qiao, G.-Y.; Yuan, S.; Pang, J.; Rao, H.; Lollar, C. T.; Dang, D.; Qin, J.-S.; Zhou, H.-C.; Yu, J. Functionalization of Zirconium-Based Metal−Organic Layers with Tailored Pore Environments for Heterogeneous Catalysis. *Angew. Chem., Int. Ed.* **2020**, *59*, 18224−18228.
(15) Fu, Z.; Shu, C.; Wang, X.; Chen, L.; Wang, X.; Liu, L.; Wang, K.; Clowes, R.; Chong, S. Y.; Wu, X.; Cooper, A. I. Fluorinated Covalent Organic Frameworks Coupled with Molecular Cobalt Cocatalysts for Efficient Photocatalytic CO_2 Reduction. *CCS Chem.* **2023**, *5*, 2290−2300.
(16) Gadzikwa, T.; Matseketsa, P. The Post-Synthesis Modification (PSM) of MOFs for Catalysis. *Dalton Trans.* **2024**, *53*, 7659−7668.
(17) Wang, Z.; Cao, L.; Hu, H.; Wang, C. Postsynthetic Modification of Metal−Organic Layers. *Acc. Chem. Res.* **2025**, *58*, 812−823.
(18) Chen, J.; Guo, J.; Lu, Z. Recent Advances in Hydrometallation of Alkenes and Alkynes via the First Row Transition Metal Catalysis. *Chin. J. Chem.* **2018**, *36*, 1075−1109.
(19) Ai, W.; Zhong, R.; Liu, X.; Liu, Q. Hydride Transfer Reactions Catalyzed by Cobalt Complexes. *Chem. Rev.* **2019**, *119*, 2876−2953.
(20) Guo, J.; Cheng, Z.; Chen, J.; Chen, X.; Lu, Z. Iron- and Cobalt-Catalyzed Asymmetric Hydrofunctionalization of Alkenes and Alkynes. *Acc. Chem. Res.* **2021**, *54*, 2701−2716.
(21) Li, B.; Chrzanowski, M.; Zhang, Y.; Ma, S. Applications of Metal-Organic Fameworks Featuring Multi-Functional Sites. *Coord. Chem. Rev.* **2016**, *307*, 106−129.
(22) Zhang, Y.; Yang, X.; Zhou, H.-C. Synthesis of MOFs for Heterogeneous Catalysis via Linker Design. *Polyhedron* **2018**, *154*, 189−201.
(23) Jati, A.; Dam, S.; Kumar, S.; Kumar, K.; Maji, B. A π-Conjugated Covalent Organic Framework Enables Interlocked Nickel/Photoredox Catalysis for Light-Harvesting Cross-Coupling Reactions. *Chem. Sci.* **2023**, *14*, 8624−8634.
(24) Fan, Y.; Kang, D. W.; Labalme, S.; Lin, W. A Spirobifluorene-Based Covalent Organic Framework for Dual Photoredox and Nickel Catalysis. *J. Am. Chem. Soc.* **2023**, *145*, 25074−25079.
(25) Zhou, Z.; Fan, Y.; Blenko, A. L.; Wang, Z.; Lin, W. Photochemically Stable Amide-Linked Covalent Organic Framework for Efficient Dual Photoredox and Copper Catalysis. *ACS Catal.* **2025**, *15*, 8724−8732.
(26) Li, L.-J.; He, Y.; Yang, Y.; Guo, J.; Lu, Z.; Wang, C.; Zhu, S.; Zhu, S.-F. Recent Advances in Mn, Fe, Co, and Ni-Catalyzed Organic Reactions. *CCS Chem.* **2024**, *6*, 537−584.
(27) Sun, X.; Li, X.; Song, S.; Zhu, Y.; Liang, Y.-F.; Jiao, N. Mn-Catalyzed Highly Efficient Aerobic Oxidative Hydroxyazidation of Olefins: A Direct Approach to β-Azido Alcohols. *J. Am. Chem. Soc.* **2015**, *137*, 6059−6066.
(28) Nikolaienko, P.; Rueping, M. Trifluoromethylselenolation of Aryldiazonium Salts: A Mild and Convenient Copper-Catalyzed Procedure for the Introduction of the $SeCF_3$ Group. *Chem.—Eur. J.* **2016**, *22*, 2620−2623.
(29) Gu, Q.-S.; Li, Z.-L.; Liu, X.-Y. Copper(I)-Catalyzed Asymmetric Reactions Involving Radicals. *Acc. Chem. Res.* **2020**, *53*, 170−181.
(30) Li, Z.-L.; Fang, G.-C.; Gu, Q.-S.; Liu, X.-Y. Recent Advances in Copper-Catalysed Radical-Involved Asymmetric 1,2-Difunctionalization of Alkenes. *Chem. Soc. Rev.* **2020**, *49*, 32−48.
(31) Zhang, Z.; Chen, P.; Liu, G. Copper-Catalyzed Radical Relay in $C(sp^3)$−H Functionalization. *Chem. Soc. Rev.* **2022**, *51*, 1640−1658.
(32) Li, N.; Li, B.; Murugesan, K.; Sagadevan, A.; Rueping, M. Visible-Light-Induced Excited-State Copper Catalysis: Recent Advances and Perspectives. *ACS Catal.* **2024**, *14*, 11974−11989.
(33) Kern, J.-M.; Sauvage, J.-P. Photoassisted C−C Coupling via Electron Transfer to Benzylic Halides by a Bis(di-imine) Copper(I) Complex. *J. Chem. Soc., Chem. Commun.* **1987**, 546−548.
(34) Reiser, O. Shining Light on Copper: Unique Opportunities for Visible-Light-Catalyzed Atom Transfer Radical Addition Reactions and Related Processes. *Acc. Chem. Res.* **2016**, *49*, 1990−1996.
(35) Zhong, M.; Pannecoucke, X.; Jubault, P.; Poisson, T. Recent Advances in Photocatalyzed Reactions Using Well-Defined Copper(I) Complexes. *Beilstein J. Org. Chem.* **2020**, *16*, 451−481.
(36) Tang, X.-J.; Dolbier, W. R., Jr. Efficient Cu-catalyzed Atom Transfer Radical Addition Reactions of Fluoroalkylsulfonyl Chlorides with Electron-Deficient Alkenes Induced by Visible Light. *Angew. Chem., Int. Ed.* **2015**, *54*, 4246−4249.
(37) Bunescu, A.; Abdelhamid, Y.; Gaunt, M. J. Multicomponent Alkene Azidoarylation by Anion-Mediated Dual Catalysis. *Nature* **2021**, *598*, 597−603.
(38) Pham, L. N.; Olding, A.; Ho, C. C.; Bissember, A. C.; Coote, M. L. Investigating Competing Inner- and Outer-Sphere Electron-Transfer Pathways in Copper Photoredox-Catalyzed Atom-Transfer Radical Additions: Closing the Cycle. *Angew. Chem., Int. Ed.* **2025**, *64*, No. e202415792.
(39) Bagal, D. B.; Kachkovskyi, G.; Knorn, M.; Rawner, T.; Bhanage, B. M.; Reiser, O. Trifluoromethylchlorosulfonylation of Alkenes: Evidence for an Inner-Sphere Mechanism by a Copper Phenanthroline Photoredox Catalyst. *Angew. Chem., Int. Ed.* **2015**, *54*, 6999−7002.
(40) Hossain, A.; Vidyasagar, A.; Eichinger, C.; Lankes, C.; Phan, J.; Rehbein, J.; Reiser, O. Visible-Light-Accelerated Copper(II)-Catalyzed Regio- and Chemoselective Oxo-Azidation of Vinyl Arenes. *Angew. Chem., Int. Ed.* **2018**, *57*, 8288−8292.
(41) Hossain, A.; Engl, S.; Lutsker, E.; Reiser, O. Visible-Light-Mediated Regioselective Chlorosulfonylation of Alkenes and Alkynes: Introducing the Cu(II) Complex $[Cu(dap)Cl_2]$ to Photochemical ATRA Reactions. *ACS Catal.* **2019**, *9*, 1103−1109.
(42) Reichle, A.; Koch, M.; Sterzel, H.; Großkopf, L.; Floss, J.; Rehbein, J.; Reiser, O. Copper(I) Photocatalyzed Bromonitroalkylation of Olefins: Evidence for Highly Efficient Inner-Sphere Pathways. *Angew. Chem., Int. Ed.* **2023**, *62*, No. e202219086.
(43) Engl, S.; Reiser, O. Making Copper Photocatalysis Even More Robust and Economic: Photoredox Catalysis with $[Cu^{II}(dmp)_2Cl]Cl$. *Eur. J. Org. Chem.* **2020**, *2020*, 1523−1533.
(44) Riesgo, E. C.; Hu, Y.-Z.; Bouvier, F.; Thummel, R. P.; Scaltrito, D. V.; Meyer, G. J. Crowded Cu(I) Complexes Involving Benzo[*h*]-quinoline: π-Stacking Effects and Long-Lived Excited States. *Inorg. Chem.* **2001**, *40*, 3413−3422.

https://doi.org/10.1021/jacs.5c17585
J. Am. Chem. Soc. XXXX, XXX, XXX−XXX

(45) Beaudelot, J.; Oger, S.; Peruško, S.; Phan, T.-A.; Teunens, T.; Moucheron, C.; Evano, G. Photoactive Copper Complexes: Properties and Applications. *Chem. Rev.* **2022**, *122*, 16365−16609.
(46) Waller, P. J.; Gándara, F.; Yaghi, O. M. Chemistry of Covalent Organic Frameworks. *Acc. Chem. Res.* **2015**, *48*, 3053−3063.
(47) Diercks, C. S.; Yaghi, O. M. The Atom, the Molecule, and the Covalent Organic Framework. *Science* **2017**, *355*, No. eaal1585.
(48) Geng, K.; He, T.; Liu, R.; Dalapati, S.; Tan, K. T.; Li, Z.; Tao, S.; Gong, Y.; Jiang, Q.; Jiang, D. Covalent Organic Frameworks: Design, Synthesis, and Functions. *Chem. Rev.* **2020**, *120*, 8814−8933.
(49) Zou, L.; Chen, Z.-A.; Si, D.-H.; Yang, S.-L.; Gao, W.-Q.; Wang, K.; Huang, Y.-B.; Cao, R. Boosting CO_2 Photoreduction via Regulating Charge Transfer Ability in a One-Dimensional Covalent Organic Framework. *Angew. Chem., Int. Ed.* **2023**, *62*, No. e202309820.
(50) Wang, L.; Wang, L.; Zhao, Q.; Ji, X.; Zhao, M.; Zhang, Y.; Lai, M. A. Pyrenetetrayl/Phenanthroline-Based One-Dimensional Covalent Organic Framework for Metal-Free Photocatalytic Organic Conversion. *J. Mater. Chem. A* **2024**, *12*, 28424−28436.
(51) Cui, M.; Wang, D.; Guo, J.; Dai, M.; Sun, M.-Y.; Li, Z.; Wun, C. K. T.; Bachmann, S.; Chow, W. Y.; Lo, T. W. B.; Zhou, M.; Xu, W. W.; He, J. Developing a Highly Reducing Heterogeneous Nickel Photocatalyst with Photoexcited Hantzsch Esters. *J. Am. Chem. Soc.* **2025**, *147*, 32982−32993.
(52) Wu, X.; Cui, M.; Wu, K.; Guo, J.; Liu, T.; Liu, D.; Li, Z.; Weng, P.; Xia, R.-Q.; Xiong, X.; Huang, Y.-L.; Li, D.; He, J. Enhancing Electron Donor−Acceptor Complex Photoactivation with a Stable Perylene Diimide Metal−Organic Framework. *J. Am. Chem. Soc.* **2025**, *147*, 8350−8360.
(53) Ghosh, I.; Ghosh, T.; Bardagi, J. I.; König, B. Reduction of Aryl Halides by Consecutive Visible Light-Induced Electron Transfer Processes. *Science* **2014**, *346*, 725−728.
(54) Zeng, L.; Liu, T.; He, C.; Shi, D.; Zhang, F.; Duan, C. Organized Aggregation Makes Insoluble Perylene Diimide Efficient for the Reduction of Aryl Halides via Consecutive Visible Light-Induced Electron-Transfer Processes. *J. Am. Chem. Soc.* **2016**, *138*, 3958−3961.
(55) Rosso, C.; Filippini, G.; Prato, M. Use of Perylene Diimides in Synthetic Photochemistry. *Eur. J. Org. Chem.* **2021**, *2021*, 1193−1200.
(56) Heckelmann, I.; Lu, Z.; Prentice, J. C. A.; Auras, F.; Ronson, T. K.; Friend, R. H.; Nitschke, J. R.; Feldmann, S. Supramolecular Self-Assembly as a Tool to Preserve the Electronic Purity of Perylene Diimide Chromophores. *Angew. Chem., Int. Ed.* **2023**, *62*, No. e202216729.
(57) Nguyen, H. L.; Gropp, C.; Yaghi, O. M. Reticulating 1D Ribbons into 2D Covalent Organic Frameworks by Imine and Imide Linkages. *J. Am. Chem. Soc.* **2020**, *142*, 2771−2776.
(58) Liu, C.; Ma, D.-L.; Tian, P.-J.; Jia, C.; Qi, Q.-Y.; Jiang, G.-F.; Zhao, X. Lateral Functionalization of a One-Dimensional Covalent Organic Framework for Efficient Photocatalytic Hydrogen Evolution from Water. *J. Mater. Chem. A* **2024**, *12*, 16063−16069.
(59) Shang, S.; Wei, Y.; Zhao, X.; Wang, W.; An, S.; Li, H.; Peng, C.; Liu, H.; Chen, H.; Hu, J. Dimensional Engineering of 1D/2D Covalent Organic Framework Isomers for Enhanced CO_2 Photoreduction. *Small* **2025**, *21*, No. e06081.
(60) Auras, F.; Ascherl, L.; Bon, V.; Vornholt, S. M.; Krause, S.; Döblinger, M.; Bessinger, D.; Reuter, S.; Chapman, K. W.; Kaskel, S.; Friend, R. H.; Bein, T. Dynamic Two-Dimensional Covalent Organic Frameworks. *Nat. Chem.* **2024**, *16*, 1373−1380.
(61) Patonay, T.; Kónya, K.; Juhász-Tóth, É. Syntheses and Transformations of α-Azido Ketones and Related Derivatives. *Chem. Soc. Rev.* **2011**, *40*, 2797−2847.
(62) Liu, M.; Fu, Y.; Bi, S.; Yang, S.; Yang, X.; Li, X.; Chen, G. Z.; He, J.; Xu, Q.; Zeng, G. Dimensionally-Controlled Interlayer Spaces of Covalent Organic Frameworks for the Oxygen Evolution Reaction. *Chem. Eng. J.* **2024**, *479*, 147682.
(63) Wang, J.; Sun, H.; Huang, S.; Duan, F.; Gu, H.; Du, M.; Lu, S. Construction of One-Dimensional Covalent−Organic Framework Coordinated with Main Group Metals for Selective Electrochemical Synthesis of H_2O_2. *ACS Appl. Mater. Interfaces* **2024**, *16*, 56459−56468.
(64) Yang, S.; He, Z.; Li, X.; Mei, B.; Huang, Y.; Xu, Q.; Jiang, Z. In/Outside Catalytic Sites of the Pore Walls in One-Dimensional Covalent Organic Frameworks for Oxygen Reduction Reaction. *Angew. Chem., Int. Ed.* **2025**, *64*, No. e202418347.
(65) He, J.; Chen, C.; Fu, G. C.; Peters, J. C. Visible-Light-Induced, Copper-Catalyzed Three-Component Coupling of Alkyl Halides, Olefins, and Trifluoromethylthiolate to Generate Trifluoromethyl Thioethers. *ACS Catal.* **2018**, *8*, 11741−11748.
(66) Forero Cortés, P. A.; Marx, M.; Trose, M.; Beller, M. Heteroleptic Copper Complexes with Nitrogen and Phosphorus Ligands in Photocatalysis: Overview and Perspectives. *Chem. Catal* **2021**, *1*, 298−338.
(67) Hussain, M. I.; Feng, Y.; Hu, L.; Deng, Q.; Zhang, X.; Xiong, Y. Copper-Catalyzed Oxidative Difunctionalization of Terminal Unactivated Alkenes. *J. Org. Chem.* **2018**, *83*, 7852−7859.
(68) Zhu, C.; Gong, C.; Cao, D.; Ma, L.-L.; Liu, D.; Zhang, L.; Li, Y.; Peng, Y.; Yuan, G. Cobalt-Metalated 1D Perylene Diimide Carbon-Organic Framework for Enhanced Photocatalytic α-C(sp^3)−H Activation and CO_2 Reduction. *Angew. Chem., Int. Ed.* **2025**, *64*, No. e202504348.
(69) Li, Y.; Jiang, H.; Zhang, W.; Zhao, X.; Sun, M.; Cui, Y.; Liu, Y. Hetero- and Homointerlocked Metal−Organic Cages. *J. Am. Chem. Soc.* **2024**, *146*, 3147−3159.
(70) Li, G.-Q.; Li, Z.-Q.; Jiang, M.; Zhang, Z.; Qian, Y.; Xiao, W.-J.; Chen, J.-R. Photoinduced Copper-Catalyzed Asymmetric Three-Component Radical 1,2-Azidooxygenation of 1,3-Dienes. *Angew. Chem., Int. Ed.* **2024**, *63*, No. e202405560.
(71) Jin, J.-K.; Wu, K.; Liu, X.-Y.; Huang, G.-Q.; Huang, Y.-L.; Luo, D.; Xie, M.; Zhao, Y.; Lu, W.; Zhou, X.-P.; He, J.; Li, D. Building a Pyrazole−Benzothiadiazole−Pyrazole Photosensitizer into Metal−Organic Frameworks for Photocatalytic Aerobic Oxidation. *J. Am. Chem. Soc.* **2021**, *143*, 21340−21349.

https://doi.org/10.1021/jacs.5c17585
J. Am. Chem. Soc. XXXX, XXX, XXX−XXX